

The effect of pH on the optical band gap of PbSe thin film with usability in the quantum dot solar cell and photocatalytic activity

Nader Ghobadi*, Parisa Sohrabi, Gholamhosain Haidari, and Seyyede Sajede Haeri

Department of Physics, Faculty of Science, Malayer University, Malayer 65719-95863, I.R. Iran

ARTICLE INFO

Article history:

Received 26 May 2019

Revised 29 June 2019

Accepted 11 August 2019

Available online 12 Aug 2019

Keywords:

Nanostructured thin films

Complex agent

Time of reaction

Quantum dot solar cell

Photocatalytic activity

ABSTRACT

This study is an attempt to provide a simple solution processed synthesis route for Lead Selenide (PbSe) nanostructure thin films using the chemical bath deposition (CBD) method which is commercially available in inexpensive precursors. In the CBD method, the preparation parameters play a considerable role to determine the nature of the final product formed. Known as two main factors, the effects of complex agent (PH) and time of reaction regarding the evolution of the configuration and the optical band gap of PbSe nanostructures with self-assemble arrays are investigated in this study. These preparation parameters were tuned to affect the nanostructured semiconductors with band gaps of around 1.4 eV where they could be used for the quantum dot solar cell. The films were characterized by X-ray diffraction (XRD), UV-visible spectroscopy for energy band gap estimation, and scanning electron microscopy (SEM) for morphology investigation as well as size distribution. The change in the pH alters the optical band gap from 3.56 to 1.4 eV. The exceptional photo-catalytic behavior from the increased visible light absorption supports the separation of photo-generated electrons and holes, where it also improves the photo-catalytic oxidizing species with PbSe nanostructured thin films.

1 Introduction

Over the recent decades, nanostructured semiconductors have gained much recognition due to their unique optical and electrical properties in comparison to the bulk materials [1]. Their electrical and optical properties are directly related to the quantum confinement of charge carriers leading to the blue shift of the band gap with a decrease in their size[2].

Several investigators have prepared PbSe thin films using different chemical methods such as spray pyrolysis [3], chemical bath deposition (CBD) [4],

photochemical deposition method [5] successive ionic layer adsorption and reaction method [6], electro deposition [7], dip and dry method [8], and vacuum evaporation [9]. The chemical bath deposition for the formation of thin films from aqueous solution is a favorable technique because of its simplicity and economically. The starting chemicals are generally available and inexpensive. This method can be used to deposit films at a low temperature which prevents oxidation of the deposited material. The deposition conditions are easily controlled to get improved orientation and grain structure of the film [10].

Moreover, the chemical bath deposition method's main advantage over the other methods is that the films on

*Corresponding author.

Email address: n.ghobadi@Malayeru.ac.ir

DOI: 10.22051/jitl.2019.26364.1032

different kinds of substrate shapes and sizes can be deposited [11]. By this method, nanostructured thin films of various semiconductors having an optical band gap controlling property have successfully been synthesized over the past years.

In the CBD method, the deposition procedure of the nanostructured materials obviously involves the procedure of deposition of a nanoparticle from the solution phase. A good comprehension of the process and preparation parameters controlling the deposition helps tailor the growth of the nanostructured thin films to the desired size and shape [2]. Then, the nanostructured semiconductor can be grown over a range of sizes, allowing them to express a variety of band gaps without changing the underlying materials or construction techniques.

The nanostructured Lead Selenide (PbSe) is an important semiconductor which has applications in optoelectronic devices [1, 2, 4], especially in quantum dot solar cell due to its enhanced photocurrent which is the result of multiple exciton generations and the ability to have the right band gap together with large exciton Bohr radius (i.e. 46 nm) [8, 12-15].

The PbSe quantum dot has the band gap that can be tuned into the infrared frequencies for the best usability in the solar cell. This range of the band gap is typically difficult to achieve with the traditional organic-inorganic solar cell. In fact, half of the solar energy reaching the earth is in the infrared spectrum. Moreover, the numerical analysis shows that the 31% efficiency of solar cell is achieved with a band gap of ~1.4 eV which corresponds to light in the nearby infrared spectrum [16-18].

The characteristics of the chemically deposited PbSe thin films by CBD strongly depend on the growth conditions. By changing the deposition key parameters such as concentration, pH, and temperature, one can control the thickness, size of nanoparticles, and the energy band gap of the obtained thin films [10]. In fact, the nano scale systems are known to show such interesting physical properties as increasing the semiconductor band gap due to electron confinement.

In this research study, we investigate the effect of the concentration of the complex agent (PH) as one of the main parameters of the CBD method on the nano-semiconductor size and shape to shed much light on the

band gap of the PbSe nano-semiconductor. What follows is a discussion of how we attempted to tune the band gap around 1.4 eV which is appropriate for making PbSe quantum dot solar cell by finding the suitable value of the pH.

The increase in pH level and the solution effect on the growth of bigger aggregates is because of the stable nuclei shaped on the substrate during the reaction leading to the formation of a contacting crystal at which two or more crystals are associated at a higher pH level. This is because the smaller crystals, which are greater in the number of high pH values, do not have sufficient amount of energy to generate coalescence, but the phenomenon of the aggregation is predictable. On the other hand, the small crystals cannot grow large like single crystals because the process is being followed by a terminating step resulting in the formation of the aggregates.

It is well-known that nanomaterial properties depend on particles size. Brus proposed a relation between the energy band gap (E_R) and particle size (R) that yields an expression for the band gap of the quantum dot [19]:

$$E_R = E_g + \left(\frac{1}{m_e^*} + \frac{1}{m_h^*} \right) \frac{\hbar^2 \pi^2}{2R^2} - \frac{1.8e^2}{\epsilon R}, \quad (1)$$

where E_g is the bulk band gap, R is the radius of the quantum dot, and ϵ is the dielectric constant. The second term is the kinetic energy term containing the effective masses of the electron and the hole (m_e^* , and m_h^* respectively). The third term arises due to the Coulomb attraction.

What follows is a summary of photo catalytic degradation activities on the famous photocatalytic. It is known that the photo catalytic degradation of pollutants over TiO_2 only proceeds under UV irradiation. Also the solar spectrum consists of only 5–7% of UV light, the other 46% and 47% of the spectrum are visible light with the wavelength between 400 and 700 nm and infrared radiation, respectively [19-21].

For practical reasons, it is necessary to develop new catalysts that are able to operate effectively under the natural sunlight. In order to utilize the sunlight, the band gap of TiO_2 has to be narrowed or splitted into several sub-gaps, which can be achieved by doping the transitional metal ions, e.g., Fe, Cu, Co, Ni or V, or by

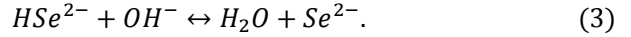
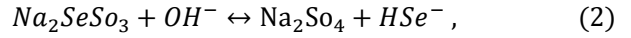
doping N [22, 23]. PbSe nanostructured thin films present the outstanding photocatalytic behavior due to the role of the increased visible light absorption, promoted separation of photo-generated electrons and holes as well as enhanced photo-catalytic oxidizing. These samples are composed of nanoparticles with different nano grain sizes, and they have different optical band gaps. Adjust yourself to the interaction with sunlight, so the PbSe nanostructured thin films are the best material for photocatalytic applications.

2 Experimental procedures

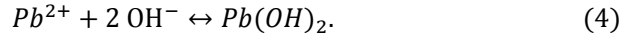
A good understanding of the deposition procedure helps control the growth of the nanoparticles to the desirable nanostructured thin film. The PbSe thin films were grown on ordinary glass slides (26 mm × 7.6 mm × 2 mm). The substrate cleaning plays an important role in the deposition of thin films. Therefore, before deposition, the substrates were washed in the detergent, rinsed in the acetone, ultrasonically cleaned and finally rinsed again with a mixture of the double distilled water and methanol. The substrates were kept in vacuum. To provide Pb^{2+} ions, 50 ml of $Pb(CH_3COO)_2$ (Lead Acetate) according to Tables 1 and 2 was taken in a glass beaker with 100 ml capacity under constant stirring, before 25% ammonia was gradually added to the solution. At first, the solution became milky where further addition of excessive ammonia made the solution white and transparent. The 50 ml of freshly prepared Sodium Selenite (Na_2SeSO_3) was gradually added to the solution. The glass substrates were vertically immersed into the deposition solution. In order to control the rate of the film's growth, the bath temperature was kept constant at the desired value. To control the complex agent, the ammonia was added to the solution which contained Pb^{2+} ions. At the end of the deposition process, all of the deposited substrates were removed from the chemical bath at suitable intervals before washed with the deionized water and methanol to remove the loosely adhered PbSe nanoparticles off the films. The coating on one side of each substrate was removed by a cotton swab moistened with dilute HCl before the films were dried in air and finally placed in the desiccators.

The formation of the PbSe thin film was based on the slow release of Pb^{2+} and Se^{2-} ions in the aqueous medium before subsequent condensation on the

substrate. The reaction mechanism involved in the deposition of the PbSe film is proposed as below [21]:

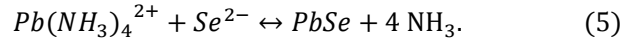


When the ammonia solution is added to the Pb^{2+} salt solution, $Pb(OH)_2$ starts precipitating when the solubility product (SP) of $Pb(OH)_2$ is exceeded, i.e.:



The $Pb(OH)_2$ precipitate dissolves in the excessive ammonia solution to form the complex lead tetra-ammine ions $Pb(NH_3)_4^{2+}$ ($Pb^{2+} + 4 NH_3 \leftrightarrow [Pb(NH_3)_4]^{2+}$).

Finally, the PbSe thin film formation takes place:



The thickness of the deposited film was measured with the help of sensitive microbalance using the relation, $t = \frac{m}{\rho A}$, where m is the mass of the deposited film, A is the area of the deposited film, and ρ is the density of the deposited material ($PbSe = 8.10 \text{ g/cm}^3$) in the bulk form.

3 Results and discussions

3.1 Optical absorption

The optical properties of PbSe thin films were investigated in room temperature using UV-Vis spectrometry (Perkin-Elmer, UV/VIS Spectrometer Lambda25-USA) in a wavelength range of 190-1100 nm to show the variation of the optical band gap with different concentration rates of the complex agent (PH). The absorbance data were analyzed using the following well-known equation for near the edge optical absorption of semiconductors [24]:

$$\alpha = B \left(h\nu - \frac{E_g}{h\nu} \right)^n, \quad (6)$$

where α is the absorption coefficient defined by the Beer-Lambert's law ($\alpha(\lambda) = \frac{2.303 \times A(\lambda)}{d}$, where d and A are respectively the film thickness and absorbance), ($h\nu$) is the photon energy, B is a constant, E_g is the optical band gap, n is a constant respectively equal to 1/2 and 2 for the allowed direct and indirect gap semiconductors [22].

In previous studies [24, 25], it has been shown that “an absorbance data for any sample has a unique optical band gap” where the supposedly different thickness doesn't change the optical band gap. In fact, the optical band gap can be determined without thickness measurement or absorption coefficient, which only requires the absorbance spectrum. On the other hand, this ineffective thickness method (ITM) used to determine the optical band gap doesn't need any presumptions and additional measurements.

The optical absorption spectroscopy is the most commonly used method for exploring quantum effects in the nanostructured semiconductor. In light of the ITM method, the optical band gap and the plot of $(Ah\nu)^2$ versus $(h\nu)$ were estimated as shown in Fig 1. Also, the specifications of the CBD method are shown in Table 1. For PbSe thin films with various pH values, the best linear fit was obtained for $n=1/2$. Moreover, Table 1 vividly indicates the calculated band gaps for distinct samples with different values of pH.

The films show a red shift in their optical band gap from 3.56eV to 1.44eV. It is obvious that the optical band gap decreases by increasing the concentration of the complex agent value. These nanocrystalline films were shown to have very strong confinement effects, as the reduction of grain size increases its energy band gap [19]. The pH of the reaction helps tailor the thin film configuration and has a basic role in the preparation of nanostructured materials.

Table 1. The energy band gap of PbSe nanoparticle films (the S series) with different pH values.

No.	Lead Acetate (mol)	Sodium Selenite (mol)	pH
S-1	0.13	0.13	12.37
S-2	0.13	0.13	12.00
S-3	0.13	0.13	11.60
S-4	0.13	0.13	10.00
S-5	0.13	0.13	9.6

No.	Deposition Temperature (°C)	Deposition Time (hour)	Optical band gap(eV)
S-1	40	24	1.44
S-2	40	24	1.47
S-3	40	24	3.46
S-4	40	24	3.48
S-5	40	24	3.56

It is evident from Table 2 that calcium ions in neodymium sites and antimony ions in arsenic sites are substituted completely. The XRD patterns of the synthesized samples that are refined by the MAUD software are presented in Figs. 2(a-c).

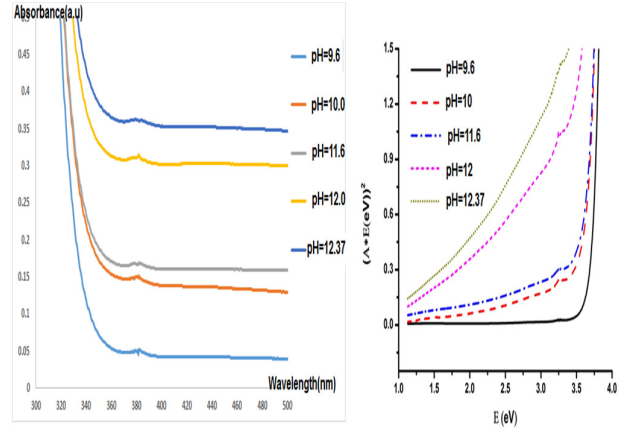


Figure 1. The plot of $(Ah\nu)^2$ versus $(h\nu)$ for the samples introduced in Table 1 (the S series samples).

By tuning the pH of the CBD method, the appropriate band gap of the nanostructured semiconductor with usability in the quantum dot solar cells can be achieved. The samples with the band gap around 1.4 eV (when the pH is around 12) are appropriate for use in the quantum dot solar cell.

To investigate the effect of the deposition time on the band gap when the pH is around 12, we changed the deposition time from 1h to 16 h. The specifications of the CBD method and the calculated band gaps are also shown in Table 2 for the A series samples. For some of the A series samples, the optical band gaps which are near 1.4 eV, the variation of the optical band gap as a function of the deposition times from 1h to 16 h is presented in Fig 2. It can be noticed from Fig 2 and Table 2 that the optical band gap is time dependent and slowly increases at lower deposition times from 1h to 3h, and is almost the same after 3h, i.e., the growth rate is very slow at higher deposition times after 3 h. It is manifest that as the deposition time increases, the optical band gaps of thin films also decreases. Lead Selenide is an important semiconductor which is an inspiring material due to its small band gap (0.27 eV) and large bulk exciton Bohr radius (46 nm). Additionally, it is revealed that the optical band gap values change from 3.65 to 1.34 as preparation parameters are controlled, see Tables 1 and 2.

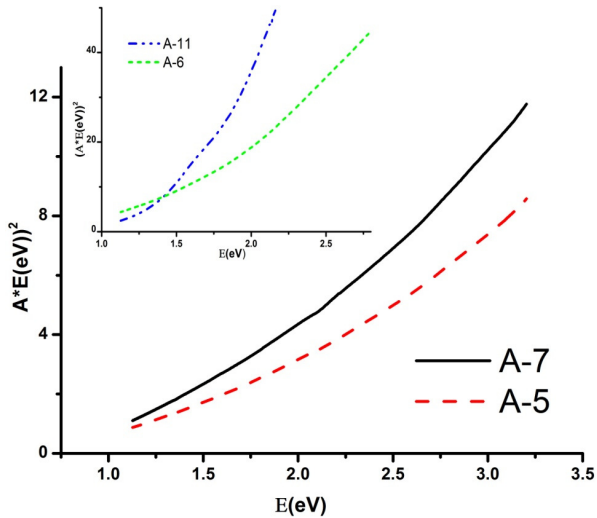


Figure 2. The plot of $(Ahv)^2$ versus (hv) for some samples of the A series.

Table 2. The Energy band gap of the PbSe nanoparticle films at different deposition times (the A series samples).

No.	Lead Acetate (mol)	Na_2SeSO_3 (mol)	pH
A-1	0.17	0.1	12.41
A-2	0.17	0.1	12.41
A-3	0.17	0.1	12.41
A-4	0.17	0.1	12.41
A-5	0.17	0.1	12.41
A-6	0.17	0.1	12.41
A-7	0.17	0.1	12.87
A-8	0.17	0.1	12.87
A-9	0.17	0.1	12.87
A-10	0.2	0.13	12.39
A-11	0.2	0.13	12.39
A-12	0.2	0.13	12.39

No.	Deposition Temperature ($^{\circ}C$)	Deposition Time (hour)	Optical band gap(eV)
A-1	RT*	1	2.45
A-2	RT	3	1.90
A-3	RT	16	1.80
A-4	40	1	1.86
A-5	40	3	1.49
A-6	40	16	1.37
A-7	RT	1	1.5
A-8	RT	3	1.49
A-9	RT	16	1.37
A-10	RT	1	1.97
A-11	RT	3	1.56
A-12	RT	16	1.34

* Room Temperature (RT)

3.2 Microstructural and XRD Studies

As shown by Fig 3, the XRD pattern of the PbSe nanostructured thin films (some of the S series samples) indicates that these samples are pure-phase compounds. The product has peaks corresponding to the hexagonal PbSe (space group: P63/mmc) phase with cell constants $a = b = 0.363$, $c = 0.530$ nm, which are in agreement with JCPDS 00-015-0464. The intense and sharp diffraction peaks suggest that the obtained product is well crystallized. Furthermore, the overall observed intensity of the peaks is quite low like that of the standard intensity indicating that the deposited material is nanocrystalline in nature. The XRD pattern of some of the S and A series samples are shown in Figs 4 and 5, respectively.

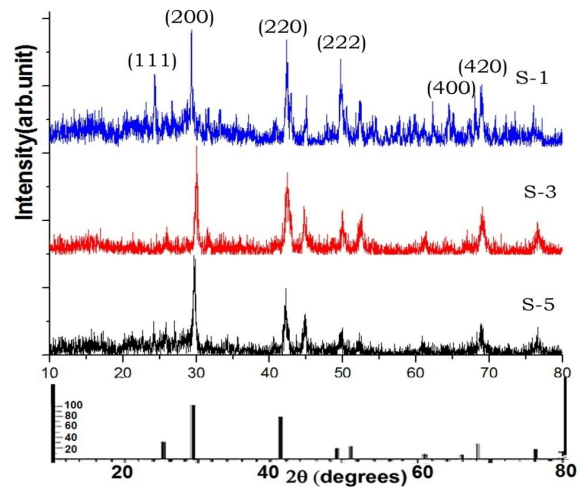


Figure 3. Representative XRD patterns of some samples of the S series.

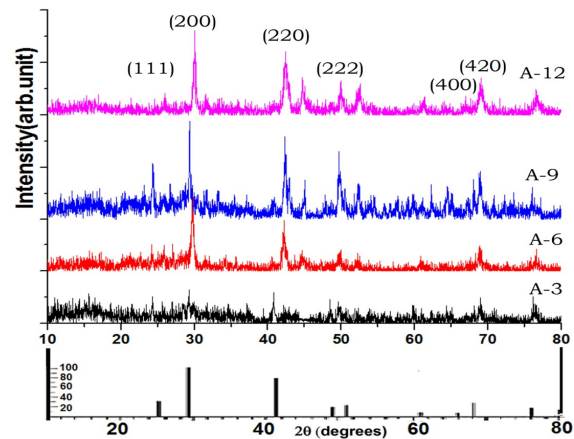


Figure 4. Representative XRD patterns of some samples of the A series.

3.3 Scanning Electron Microscopy (SEM)

The SEM images (as indicated by Fig 5) show evolution in size of the particle and the morphology of the nanostructured thin films by the concentration of the changing complex agent (the S series samples). The pH plays a crucial role in the deposition process. The grain growth of the PbSe thin film along with an increase in the pH of the chemical bath is observed to be due to the aggregation phenomenon. It is seen that bigger particles are formed by increasing the pH rate. The S-5 Sample has a pH equal to 9.6 and is composed of the nanoparticle that is much smaller than the other samples. The energy band gap of this sample is 3.56 eV showing that there exists a very strong confinement effect, as the reduction of the grain size increases its energy band gap.

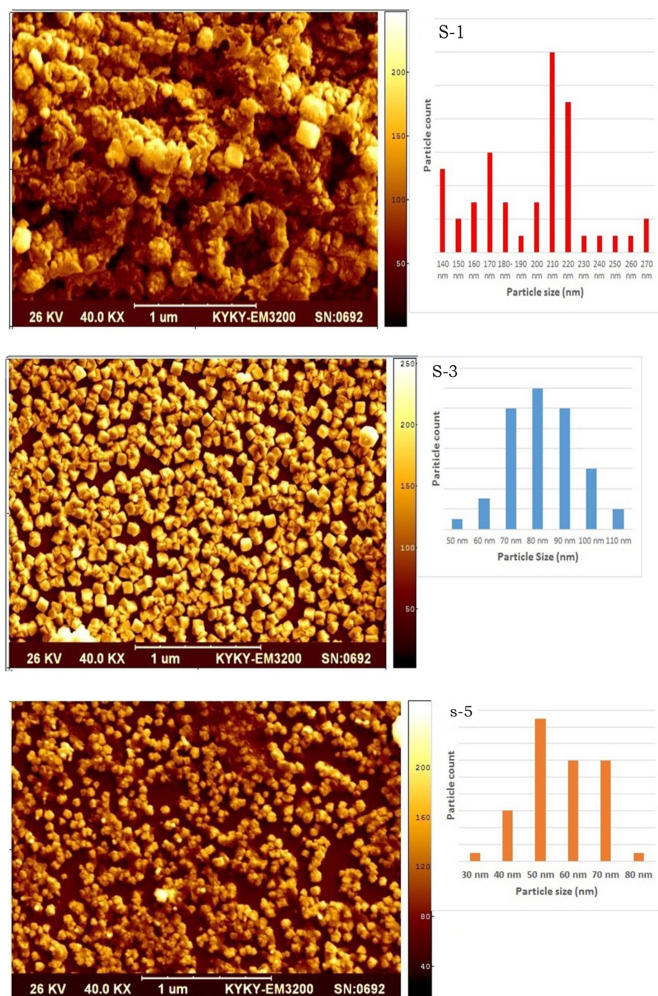


Figure 5. SEM images of some samples of the S series.

The increase in the pH rate of the solution results in the formation of the bigger aggregates because of the stable nuclei formed on the substrate during the reaction leading to the formation of a contacting crystal with which two or more crystals are associated at the higher pH value of the solution. This is because of the smaller crystals, which are greater than the number of the high pH values. Moreover, the size distribution of the nanostructured-semiconductor for the S1 sample is much wider than the other samples. Because of the different range size of the nanostructured-semiconductor, there are different band gaps. Hence in the absorption spectrum, the slope of the curve of these kinds of samples has a milder slope than the others.

3.4 Photo-Catalytic Activity Measurement

The photo-catalytic reaction of Lead Selenide nanostructured thin films was estimated by aqueous Congo red solution under visible light. The visible irradiation was provided by a 30 W LED lamp. The petri dish filled with Congo red solution (2×10^{-6} M, 30ml) and (4 Cm \times 2.5 Cm) PbSe nanostructured thin films were placed about 5 Cm from the lamp. At a given irradiation time (15 min), the samples were taken out and analyzed by UV-Visible spectrophotometer (PerkinElmer, Lambda 25), using DI water as the reference.

The intensity of the Congo red characteristic band at 500 nm (I500: the main absorption band of Congo red) in the obtained UV-Vis spectrum was, as shown by Fig 7, used to determine the absorption of the Congo red in the solution (A_t). The degradation efficiency of the Congo red, which represents the photo-catalytic efficiency of the nanoparticles, can be determined by Eq. (5)

$$\eta(\%) = (A_0 - A_t)/A_0 \times 100, \quad (7)$$

where η is the degradation efficiency, A_t is absorption after radiation, and A_0 is absorption before radiation [26].

After 165 minutes of LED irradiation, η reaches 6.8%. The mechanism of photocatalytic activity of the PbSe thin film is illustrated in Fig 6.

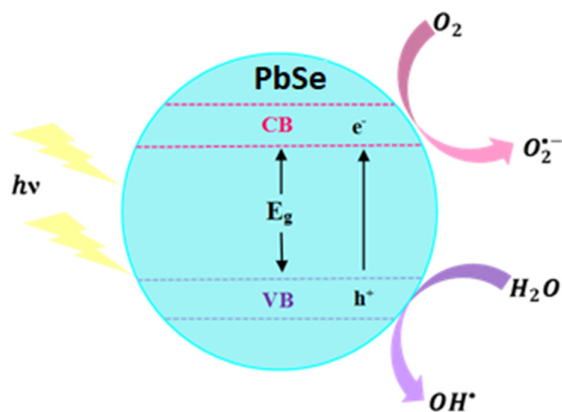


Figure 6. Schematic diagram of photocatalytic activity.

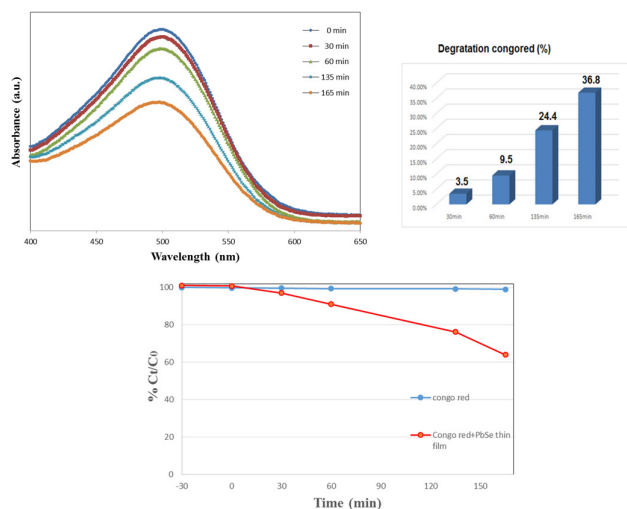


Figure 7. Photo-catalytic decomposition profile of Congo red for sample S1 after 165 minutes LED irradiation

Also, Fig 8 shows the degradation of the Congo red during UV illumination ($\lambda=356$ nm). All of the parameters of the investigation were similar to the previous photo-catalytic degradation of the Congo red under Vis light irradiation. As can be seen, the degradation efficiency of the Congo red increased along with the UV irradiation and after 150 minutes reaches 67.7%.

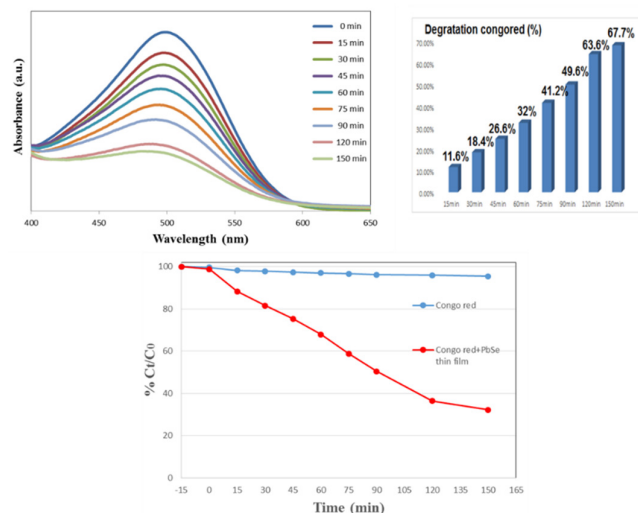


Figure 8. The Photo-catalytic decomposition profile of Congo red for sample S1 after 150 minutes UV irradiation

4 Conclusions

PbSe nanostructured thin films were, in this study, prepared using the chemical solution deposition method. To obtain the appropriate band gap (i.e., the band gap around 1.4 eV with a high level of usability in the quantum dot solar cells), the effects of the pH and time of reaction were studied.

From the present study aimed at producing the appropriate PbSe thin films, which can be used in the quantum dot solar cell, the following conclusions can safely be drawn:

- (1) The homogenous films made up of nanoparticle structures have a hexagonal structure.
- (2) The films obtained from this study are rather adherent and uniform, as observed by the naked eye and SEM images.
- (3) We investigated the concentration of the complex agent effect (pH) that governs the evolution of the thin film configurations in Pb Senanstructured arrays. The concentration of the complex agent (pH) effect has a critical role in the fabrication of the thin layers of high quality with desired features. The increase of the concentration of complex agent of the reaction solution results in the formation of bigger and wider aggregates as well as a more widely- sized distribution.

- (4) The increase of the semiconductor band gap due to the decrease in the size and products vividly shows strong electron confinement inside the nanoparticle boundaries. The direct band gap of the resulting nanoparticles can be tuned especially for use in the quantum dot solar cell by altering the nanocrystal size.
- (5) The photo-catalytic experiment revealed that PbSe nanostructured thin films were evaluated by the photocatalytic degradation kinetics of the aqueous Congo red under ultraviolet and visible radiation. The results yielded from this study show that the photocatalytic activity under visible radiation nanostructured thin films has a 36.8% degradation efficiency. Under ultraviolet radiation, it enjoys a 67.7% degradation efficiency.

References

- [1] P. Granitzer, and K. Rumpf, "Nanostructured Semiconductors: From Basic Research to Applications." Pan Stanford Publishing, 2014.
- [2] G. C. Yi, "Semiconductor Nanostructures for Optoelectronic Devices: Processing, Characterization and Applications." Springer Berlin Heidelberg, 2012.
- [3] B. Thangaraju, and P. Kaliannan, "Spray pyrolytically deposited PbS thin films." *Semiconductor Science and Technology*, **15** (2000) 849.
- [4] D. N. Gujarathi, and J. V. Dhanvij, *Electrical and Optical Properties Of Lead Selenide Thin Films By Chemical Bath Deposition*.
- [5] E. M. El-Menyawy, G. M. Mahmoud, R. S. Ibrahim, F. S. Terra, H. El-Zahed, I. K. El Zawawi, "Structural, optical and electrical properties of PbS and PbSe quantum dot thin films." *Journal of Material Science: Materials in Electronics*, **27** (2016) 10070.
- [6] K. C. Preetha, T. L. Remadevi, "Band gap engineering in PbSe thin films from near-infrared to visible region by photochemical deposition." *Journal of Material Science: Materials in Electronics*, **25** (2014) 1783.
- [7] T. S. Bhat, S. A. Vanalakar, R. S. Devan, S. S. Mali, S. A. Pawar, Y. R. Ma, C. K. Hong, J. H. Kim, and P. S. Patil, "Compact nanoarchitectures of lead selenide via successive ionic layer adsorption and reaction towards optoelectronic devices," *Journal of Materials Science: Materials in Electronics*, **27** (2016) 4996.
- [8] Z. Hens, E. S. Kooij, G. Allan, B. Grandidier, and D. Vanmaekelbergh, "Electrodeposited nanocrystalline PbSe quantum wells: synthesis, electrical and optical properties," *Nanotechnology*, **16** (2005) 339.
- [9] S. J. Kim, and S. U. o. N. Y. a. B. E. "Engineering, Nanostructured Photovoltaic Devices for Next Generation Solar Cell." State University of New York at Buffalo, 2008.
- [10] S. Kumar, T. P. Sharma, M. Zulfequar, and M. Husain, "Characterization of vacuum evaporated PbS thin films." *Physica B: Condensed Matter* **325** (2003) 8.
- [11] D. Lincot, G. Hodes, and E. S. E. Division, "Chemical Solution Deposition of Semiconducting and Non-metallic Films: Proceedings of the International Symposium." Electrochemical Society, 2006.
- [12] R. S. Mane, and C. D. Lokhande, "Chemical deposition method for metal chalcogenide thin films." *Materials Chemistry and Physics* **65** (2000) 1.
- [13] J. J. Choi, Y.-F. Lim, M. E. B. Santiago-Berrios, M. Oh, B.-R. Hyun, L. Sun, A. C. Bartnik, A. Goedhart, G. G. Malliaras, H. D. Abruña, F. W. Wise, and T. Hanrath, "PbSe Nanocrystal Excitonic Solar Cells." *Nano Letters* **9** (2009) 3749.
- [14] P. V. Kamat, "Quantum Dot Solar Cells. Semiconductor Nanocrystals as Light Harvesters." *The Journal of Physical Chemistry C*, **112** (2008) 18737.
- [15] W. Ma, J. M. Luther, H. Zheng, Y. Wu, and A. P. Alivisatos, "Photovoltaic Devices Employing Ternary PbS_xSe_{1-x} Nanocrystals." *Nano Letters*, **9** (2009) 1699.
- [16] H. Dang, "Nanostructured Semiconductor Device Design in Solar Cells." University of Kentucky, 2015.
- [17] E. H. Sargent, "Infrared Quantum Dots." *Advanced Materials*, **17** (2005) 515.
- [18] K. Mertens, "Photovoltaics: Fundamentals, Technology and Practice." Wiley, 2013.

- [19] J. Zhang, J. Gao, C. P. Church, E. M. Miller, J. M. Luther, V. I. Klimov, and M. C. Beard, "PbSe Quantum Dot Solar Cells with More than 6% Efficiency Fabricated in Ambient Atmosphere." *Nano Letters*, **14** (2014) 6010.
- [20] L. Brus, "Quantum crystallites and nonlinear optics." *Applied Physics A*, **53** (1991) 465.
- [21] G. Hodes, "Chemical Solution Deposition Of Semiconductor Films." Taylor & Francis, 2002.
- [22] J. Tauc, and A. Menth, "States in the gap." *Journal of Non-Crystalline Solids*, **8** (1972) 569.
- [23] N. Ghobadi, M. Ganji, C. Luna, A. Arman, A. Ahmadpourian, "Effects of substrate temperature on the properties of sputtered TiN thin films." *Journal of Material Science: Materials in Electronics*, **27** (2016) 2800.
- [24] N. Ghobadi, M. Ganji, C. Luna, A. Arman, A. Ahmadpourian, "The effects of DC power on the physical properties and surface topography of sputtered TiN nanostructured thin films." *Optical and Quant Electron*, **48** (2016) 467.
- [25] N. Ghobadi. "Derivation of ineffective thickness method for investigation of the exact behavior of the optical transitions in nanostructured thin films." *Journal of Material Science: Materials in Electronics*, **27** (2016) 8951.
- [26] JinKuang Dong, Haiyan Xu, FengJun Zhang, Chen Chen, Li Liu, GuoTian Wu, "Synergistic effect over photocatalytic active Cu₂O thin films and their morphological and orientational transformation under visible light irradiation." *Applied Catalysis A: General* **470** (2014) 294.